

Fabrication of glycerol liquid droplet array by nano-inkjet printing method

Kiyohiro Kaisei, Kei Kobayashi, Kazumi Matsushige, and Hirofumi Yamada

Citation: *J. Appl. Phys.* **111**, 074319 (2012); doi: 10.1063/1.3699388

View online: <http://dx.doi.org/10.1063/1.3699388>

View Table of Contents: <http://jap.aip.org/resource/1/JAPIAU/v111/i7>

Published by the [American Institute of Physics](#).

Related Articles

Room temperature ferroelectric and magnetic investigations and detailed phase analysis of Aurivillius phase Bi₅Ti₃Fe_{0.7}Co_{0.3}O₁₅ thin films

J. Appl. Phys. **112**, 052010 (2012)

Terahertz transmission characteristics across the phase transition in VO₂ films deposited on Si, sapphire, and SiO₂ substrates

J. Appl. Phys. **112**, 033523 (2012)

Study of barrier inhomogeneities in I–V–T and C–V–T characteristics of Al/Al₂O₃/PVA:n-ZnSe metal–oxide–semiconductor diode

J. Appl. Phys. **112**, 024521 (2012)

Laser-assisted sol-gel growth and characteristics of ZnO thin films

Appl. Phys. Lett. **100**, 252108 (2012)

Ultra-sharp metal and nanotube-based probes for applications in scanning microscopy and neural recording

J. Appl. Phys. **111**, 074703 (2012)

Additional information on *J. Appl. Phys.*

Journal Homepage: <http://jap.aip.org/>

Journal Information: http://jap.aip.org/about/about_the_journal

Top downloads: http://jap.aip.org/features/most_downloaded

Information for Authors: <http://jap.aip.org/authors>

ADVERTISEMENT



Special Topic Section:
PHYSICS OF CANCER

Why cancer? Why physics? [View Articles Now](#)

Fabrication of glycerol liquid droplet array by nano-inkjet printing method

Kiyohiro Kaisei,¹ Kei Kobayashi,² Kazumi Matsushige,¹ and Hirofumi Yamada^{1,a)}

¹Department of Electronic Science and Engineering, Kyoto University, Nishikyo-ku, Kyoto 615-8510, Japan

²Office of Society-Academia Collaboration for Innovation, Kyoto University, Yoshida Honmachi, Sakyo-ku, Kyoto 606-8501, Japan

(Received 22 November 2011; accepted 1 March 2012; published online 13 April 2012)

We have studied a local deposition method based on dynamic-mode AFM using a hollow tip with an aperture. In this method, liquid droplets are deposited onto a conductive substrate through the aperture by applying an electric voltage pulse and are imaged using the same AFM tip immediately after the deposition. In this study, we applied this method to local deposition of a glycerol solution, which can be utilized in the printed electronics and the biosensor fabrication technology. The solution in the hollow was covered with a hydrophobic ionic liquid with an extremely low vapor pressure to prevent the evaporation of the solution because the quick evaporation heavily affected the dynamic-mode AFM operation. We succeeded in the stable deposition of an array of ultrasmall droplets, which contained an added salt and possible involatile residues in the glycerol solution. © 2012 American Institute of Physics. [<http://dx.doi.org/10.1063/1.3699388>]

I. INTRODUCTION

Deposition of ultrasmall liquid droplets has attracted much attention because of the development of the printed electronics¹ as well as the biosensor fabrication technology.² There have been a large number of studies on the fundamental behavior of the liquid droplets, such as their evaporation^{3–5} and wettability.^{6–14} Depending on the purpose, an optimal deposition method can be used from various techniques: microsyringe,¹⁴ microspotting,² inkjet printing technique,¹⁵ and electrospray technique.^{16,17} An atomic force microscope (AFM) tip was also used as a local deposition tool.^{18,19} Recently a deposition method using a hollow tip with an aperture at the apex of the AFM tip was also developed.^{20,21} The droplets can be easily deposited by the contact of the tip with the substrate surface by these AFM-based techniques, which are convenient tools for the local deposition of small droplets and/or functional materials such as metal nanoparticles, DNA/RNAs, and proteins. However, the deposited droplet volume and shape can be strongly affected by the various surface conditions such as surface roughness and interfacial energy between the liquid and the surfaces of both tip and substrate.^{22–25} They also depend on the solubility of the sample molecules to be deposited.^{26,27}

We developed a local deposition technique (referred to as nano-inkjet printing method) based on dynamic-mode AFM using a non-volatile ionic liquid.²⁸ In our previous study, the droplets with a volume ranging from zepto (10^{-21}) liter to yocto (10^{-24}) liter were deposited onto a conductive surface. We also fabricated thin films with a thickness of several nanometers by depositing the zeptoliter droplets with a small spacing less than 100 nm.^{29,30} The technique can be applied to the deposition of the colloids containing metallic particles to fabricate metallic lines with a linewidth of several dozen nanometers so that the size in the printed electronics, where the minimum linewidth is still on a micrometer scale,¹⁵ can be drastically

reduced. However, an ionic liquid is scarcely used as a solvent for such local deposition.

In this study, the nano-inkjet printing method was so improved that a volatile glycerol solution was used. Since the glycerol solution can dissolve various functional materials such as metal nanoparticles, DNA/RNAs, and proteins, the fabrication allows us to fabricate the organic/polymer transistors¹ and the DNA/protein arrays.²

II. EXPERIMENTAL

Local deposition was performed using a commercial AFM instrument (SPA300/NanoNavi Station, SII NanoTechnology) and a commercial cantilever (OMCL-HA100WS, Olympus) modified by a focused ion beam (SMI-2050MS, SII NanoTechnology). The modified cantilever with an aperture had an approximate 1 pL hollow, in which a sample solution was loaded by using a dipped glass capillary. We deposited droplets by applying an electric voltage pulse between the backside coating and a conductive surface after bringing the tip in close proximity of the surface.

We used a silicon nitride cantilever having the spring constant of 15 N/m, the resonance frequency of 160 kHz, and Au/Cr backside coating. In our previous studies^{28–30} we used an ionic liquid with an extremely low vapor pressure so that we succeeded in the deposition using the aperture located in the vicinity of the AFM tip. On the other hand, in this study using an ordinary solvent, we made the aperture at the apex of the AFM tip to reduce the evaporation of the solvent during the deposition because the vapor pressure of the solvent is much larger than that of an ionic liquid. The aperture was opened by irradiating an ion beam at the hollow bottom, the location of which corresponded to the apex of the AFM tip on the opposite side. Typical modification parameters were the accelerating voltage of 30 kV, the probe current of 200 pA, the ion dose of 10^{13} m⁻², and the irradiation diameter of 500 nm. Although we made the aperture at the tip apex, we were able to image the deposited droplets

^{a)}Electronic mail: h-yamada@kuee.kyoto-u.ac.jp. Telephone: +81-75-383-2307. FAX: +81-75-383-2308.

using a protrusion at the edge of the aperture. Actually, the protrusion was used as an AFM tip immediately after the deposition. The topographic image was not deteriorated even when the cantilever held the sample solution. The square region at the center of the cantilever hollow was modified to expose the SiN surface to wet the solution. Before loading the solution, the cantilever hollow was cleaned by using a UV-ozone cleaner for 10 min. When we loaded a solution with a density of $1.2 \times 10^{13} \text{ kg/m}^3$ onto the cantilever, the resonance frequency was shifted by approximately 10 kHz. The measured resonance frequency shift agreed with that estimated from the volume in the hollow.³¹

The cantilever was vibrated at a frequency close to its resonance frequency. The tip-sample distance was regulated by maintaining the vibration amplitude with a set point in amplitude modulation AFM. The vibration amplitude of the tip was approximately 20 nm peak-to-peak and the set point ratio (the ratio of the set point amplitude to the free amplitude) was 0.60 when imaging droplets and 0.14 when depositing droplets. The lower set point allowed the deposition due to a smaller tip-sample distance. The tip-sample distance feedback was turned off for the interval from 1 s before the onset of the voltage pulse to 1 s after the pulse to reduce the complicated movement of the tip during the application of the voltage pulses.²⁸ The step to turn off the feedback is important to the local deposition. In our previous study, it was found that the creation of the meniscus between the tip and sample played a major role in the local deposition. If the tip-sample distance feedback is being activated during the application of the voltage pulse, the creation of the meniscus can be suppressed. In the cantilever holding the sample solution in the hollow, the solution surface in the aperture should be a spherical cap with a curvature radius determined by the Laplace pressure of the solution in the hollow.^{20,32} We imaged the deposited droplets reproducibly, which suggested that the capillary neck was not formed between the solution surface and the sample surface.

We used glycerol as a solvent, which has a low vapor pressure of 0.6 Pa on a macroscopic scale. However, it evaporates shortly within a few hours because of a large surface area to volume ratio of a few picoliters droplet filled in the cantilever hollow. In this study, a glycerol (Nakarai Tesque) solution in the hollow was coated with a hydrophobic liquid with an extremely low vapor pressure to prevent the evaporation of the glycerol solution. In the deposition experiments,

the glycerol solution contained 0.99 mL glycerol and 10 μL 1 M ammonium nitrate (Nakarai Tesque) aqueous solution. The hydrophobic liquid used was an ionic liquid, 1-octyl-3-methyl-imidazolium hexafluorophosphate (Acros organics). It was completely separated from the glycerol solution (not shown). Each liquid was loaded in the cantilever hollow by using a dipped glass capillary, as shown in Figs. 1(b)–1(d). Figures 1(e)–1(g) show the cross-sectional schematics at the dashed white line shown in Figs. 1(b)–1(d). As shown in Fig. 1(b), the loaded volume was occasionally excessive for the subsequent loading of the hydrophobic ionic liquid. We removed the excessive glycerol solution by using a glass capillary to adjust the volume so as to fill the cantilever hollow with the glycerol solution, as shown in Fig. 1(c). After the adjustment of volume of the glycerol solution, it was subsequently coated with the hydrophobic ionic liquid, as shown in Fig. 1(d).

We used an ultrasmooth conductive surface: a Pt film with the thickness of 4 nm, which was deposited on an annealed Al_2O_3 (0 0 0 1) substrate³³ by RF sputtering. The deposition and imaging of the droplets were performed in a nitrogen environment to reduce the capillary force acting between the AFM tip and the sample surface.

III. RESULTS AND DISCUSSION

A. Liquid coating to prevent the solvent evaporation

We investigated the effect of the liquid coating using the hydrophobic ionic liquid, as shown in Figs. 2 and 3. Figure 2 shows a graph of the resonance frequency of the cantilever holding the glycerol solution without the liquid coating as the function of the elapsed time immediately after loading the solution onto the cantilever. It can be clearly seen that the resonance frequency shifts by approximately 0.2 kHz min^{-1} before 90 min after loading the glycerol solution. This is because the loaded glycerol solution decreased due to the evaporation of the glycerol. Figure 3 shows the result of using the cantilever holding a dye solution with the liquid coating. The dye solution contains 0.98 mL glycerol, 10 μL 1 M ammonium nitrate aqueous solution, and 10 μL 1.32 mM cyanine 3 bihexanoic acid dye (Sigma Aldrich) aqueous solution. In this experiment, we did not remove the Au coating of the cantilever hollow. Figs. 3A(1)–(6) show the bright-field (left images) and fluorescence images (right images). Fig. 3B shows a graph of the resonance frequency as a function of the

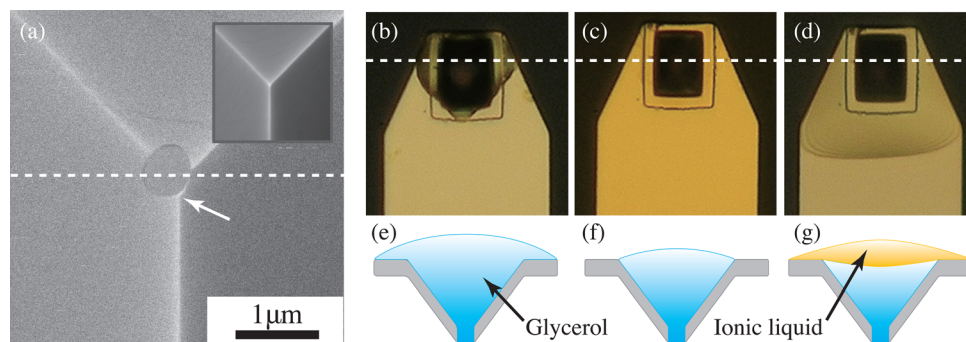


FIG. 1. (a) Scanning ion microscope image of the fabricated aperture. The inset image shows the AFM tip before the modification. The white arrow indicates a protrusion, which is the AFM tip. (b)–(d) Photographs of the cantilever hollow when coating a glycerol solution with a hydrophobic ionic liquid. (b) Glycerol solution is excessively loaded, (c) adjusted to fill the hollow, and (d) coated with the hydrophobic ionic liquid. (e)–(g) Cross-sectional schematics of the cantilever hollow at the broken white line shown in (a) correspond to each condition shown in (b)–(d).

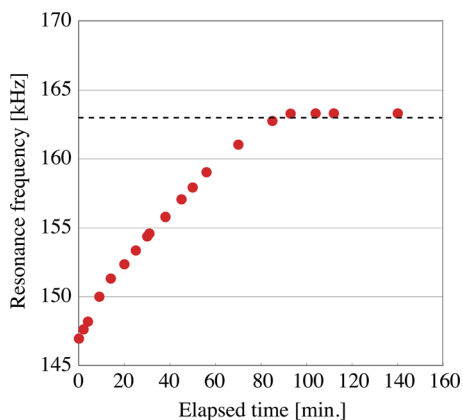


FIG. 2. Resonance frequency curve as a function of the elapsed time after loading the glycerol solution in the hollow. The dashed line shows the resonance frequency of the cantilever before loading the glycerol solution.

elapsed time. In the fluorescence images, the dashed white lines indicate the shape of the cantilever. The bright-field and fluorescence images were taken using a fluorescence microscope (BX-51, Olympus) equipped with an excitation filter (BP530-550), an absorption filter (BA575IF), a dichroic mirror (DM570), and a mercury lamp. As shown in Fig. 3A(1), the loaded glycerol droplet on the cantilever can be seen in the bright-field image, the shape of which corresponds to that of the fluorescence from the dye in the fluorescence image, thereby showing the location of the glycerol solution from each fluorescence image at different points. Even if the sol-

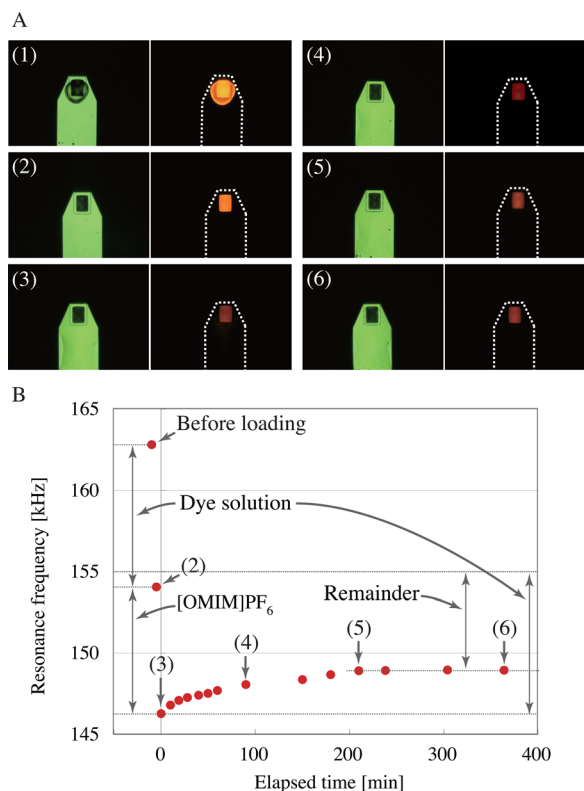


FIG. 3. A. Bright-field and fluorescence images of the cantilever holding the glycerol solution. B. Resonance frequency curve as a function of the elapsed time from loading the glycerol solution to the saturation of the frequency shift. The numerals in the graph indicate the corresponding bright-field and fluorescence images shown in A.

vent completely evaporates from the hollow, the dye remains in the hollow. However, the fluorescence from the dye cannot be observed in the experiment because the excited dye on the Au coating of the hollow is quenched. Actually, prior to this experiment, we verified that the fluorescence from the micrometer-size droplet of the dye solution on the Au coating gradually disappeared because the solvent of the dye solution evaporated from the Au coating. This result suggested that the fluorescence from the dye solution residue on Au coating was not observed. As shown in Fig. 3A(1), the dye solution was excessively loaded. The excessive dye solution was removed by a glass capillary, as shown in Fig. 3A(2). After the adjustment of volume of the dye solution, the measured resonance frequency was approximately 154 kHz (see the arrow labeled as (2) in Fig. 3B). Before loading, the measured resonance frequency was approximately 163 kHz (see the arrow labeled “Before loading” in Fig. 3B). Thus, the frequency shift caused by adding the dye solution was found to be approximately 9 kHz, which corresponded to the loaded volume (1.4 pL). After the subsequent coating of the dye solution in the hollow where the hydrophobic ionic liquid was performed, the measured resonance frequency was approximately 146 kHz (see the arrow labeled as (3) in Fig. 3B). As shown in Fig. 3A(3), it was found that the glycerol solution was coated with the hydrophobic ionic liquid. However, the resonance frequency shifted by 3 kHz to 149 kHz 210 min after loading the hydrophobic ionic liquid (see the arrow labeled as (5) in Fig. 3B). This is probably because part of the glycerol solution evaporated, which might be caused by an unintendedly uncoated glycerol solution. In each image shown in Figs. 3A(4)–3A(6), the fluorescence from the dye was observed so that the glycerol solution with the volume corresponding to approximately 6 kHz (0.9 pL) should have remained in the hollow for the deposition. Note that the evaporation of the glycerol solution through the aperture was negligible because the cross-sectional area of the aperture was much smaller than that of the hollow, which contributed to the stable dynamic mode AFM operation.

B. Deposition using the glycerol solution without the liquid coating

The deposition using the glycerol solution without the liquid coating was successfully demonstrated, as shown in Fig. 4. A voltage of 9.0 V with a duration of 5.0 s was used to fabricate a 5×5 array of droplets; the topographic image of the droplets was taken by using the same AFM tip after waiting for the complete evaporation of the solution in the hollow. The cross-sectional image of the droplets at the white line A–B has a mean height of 4.0 nm with a standard deviation of 0.45 nm and a mean diameter of 91 nm with a standard deviation of 14 nm; thus, the droplet volume was estimated to be 27 zL with a standard deviation of 11 zL, assuming that the droplets are cylindrical. The calculated volume, however, was overestimated because the mean curvature radius of the protrusion as an AFM tip was probably larger than that of commercial AFM tips. The deposited droplet should consist of the added electrolyte and the involatile residues of the glycerol because even the micrometer-size droplets evaporate in a

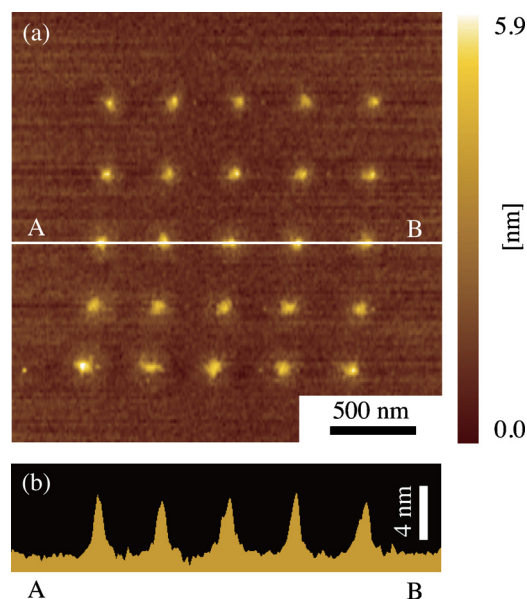


FIG. 4. (a) Topographic image of a 5×5 array of the droplets deposited by using a 9.0 V pulse with the duration of 5.0 s. (b) Cross-sectional image at the white line A–B shown in (a).

few seconds in an ambient environment.²⁴ We succeeded in the deposition of the glycerol solution in dynamic-mode AFM. However, the precise control of the deposition by using the procedure described above was difficult during the deposition process because the continuous evaporation of the solvent, overall mass change of the cantilever holding the solution, prevented the tip-sample distance regulation. Note that the solution concentration also increased with the evaporation, leading to the coalescence of solutes.

C. Deposition using the glycerol solution with the liquid coating

We show the deposition result using the glycerol solution with the liquid coating. The deposition was performed after the saturation of the resonance frequency shift was observed. We imaged the deposited droplets immediately after each deposition using the same AFM cantilever, whose hollow was still filled with the solution. The typical deposition pattern using a 9.0 V pulse with a duration of 5.0 s is shown in Fig. 5(a). The volume variation in a 10×10 array of the droplet was found to be so small that the stable deposition was achieved. As shown in Fig. 5(b), the cross-sectional image was obtained at the white line shown in Fig. 5(a). It was found that the mean height of the deposited droplets using a duration of 5.0 s at a fixed amplitude of 9.0 V were 0.78 nm with a standard deviation of 0.21 nm, while their volume was estimated to be 0.91 zL with a standard deviation of 0.49 zL, supposing their droplet structure to be cylindrical, as mentioned above. We obtained the results using different durations at fixed amplitude and found that the droplet height monotonically increased according to the pulse duration increase, as shown in Fig. 5(c). Compared with the former result without the liquid coating, the deposited droplet volume in the former result was larger than that in this result. We speculated it was due to the surface of the

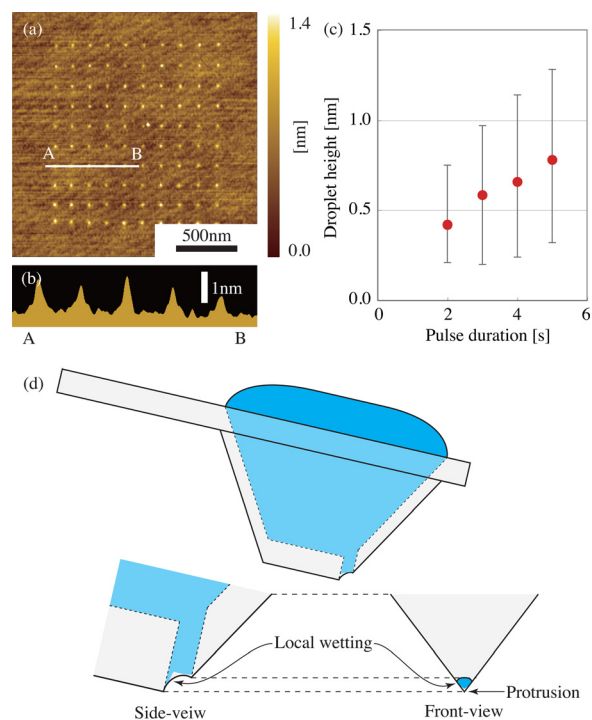


FIG. 5. (a) Topographic image of a 10×10 array of the droplets deposited by using a 9.0 V pulse with the duration of 5.0 s. (b) Cross-sectional image at the white line A–B shown in (a). (c) Droplet height against pulse durations using a 9.0 V pulse. (d) Schematics of the vicinity of the aperture.

glycerol solution in the aperture by the differences in the surface energy in the vicinity of the aperture and in the Laplace pressure of the glycerol solution in the hollow between the two cantilevers. The detailed mechanism of the local deposition is discussed in the following.

D. Discussion

In our previous studies,^{28–30} the local deposition of the ionic liquid was strongly related in the meniscus bridge between tip/aperture and surface. In dynamic-mode AFM, the meniscus bridge, affecting the resonance of the cantilever, cannot be created without applying an electric voltage pulse with an amplitude that was larger than a threshold voltage.^{34,35} This meniscus bridge allows the local deposition. It was observed that the tip vibration was suppressed due to the meniscus bridge in a nitrogen environment.

The local deposition using the glycerol solution, as shown in Figs. 4 and 5, might be caused by the similar phenomenon to that in our previous studies. The deposition volume of each study was independent of the aperture diameter and each deposition position was located at each tip position, which suggested that the outlet of the deposition in this study was also locally confined in the vicinity of the protrusion as the AFM tip.²⁸ In our previous studies, we ascribed the creation of the zeptoliter or less ionic liquid droplets to the local deposition via a small reservoir of the ionic liquid in the vicinity of an AFM tip. The reservoir was connected to the liquid in the aperture. Note that it is important to pay attention to the tip-aperture distance of several hundred nanometers in terms of the control of the local deposition. Because in this study we made an array of the zeptoliter or less droplets with

a spacing that was much less than the aperture diameter without droplet coalescence, it was naturally concluded that the meniscus bridge was limited to a local area on the sample surface, as reported by Fang *et al.*²⁴ It also suggested that the liquid on only a part of the inner surface of the aperture, as shown in Fig. 5(d), extended toward the sample surface and contributed to the local deposition. Thus, one of the important factors for achieving a reproducible deposition is the control of the end of the solution on the inner surface of the aperture, which is difficult at present because it can be affected by various causes such as electrowetting phenomenon^{36,37} and the evaporation of the solvent. Further mechanism of the local deposition will be investigated in the future.

Moreover, we recently applied this method to the local deposition of a glycerol solution including Au colloids with a diameter of 10 nm with the aim of fabricating metallic wires^{15,38} and biological sensors.^{2,16}

IV. CONCLUSIONS

We succeeded in the local deposition of zeptoliter or less glycerol solution, which contained only an added salt and the involatile residues of the solvent, by using the nanoinkjet printing method. It was found that the stable deposition was performed by coating the glycerol solution with the hydrophobic ionic liquid even when dynamic-mode AFM was used. Moreover, the deposited droplets were imaged by using the same AFM tip immediately after the deposition.

ACKNOWLEDGMENTS

This work was supported by Grants-in-Aid for Scientific Research from the Ministry of Education, Culture, Sports, Science and Technology of Japan and Global COE Program of the Japan Society for the Promotion of Science.

- ¹W. Clemens, W. Fix, J. Ficker, A. Knobloch, and A. Ullmann, *J. Mater. Res.* **19**, 1963 (2004).
- ²M. Schena, D. Shalon, R. W. Davis, and P. O. Brown, *Science* **270**, 467 (1995).
- ³R. G. Picknett and R. Bexon, *J. Colloid Interface Sci.* **61**, 336 (1977).
- ⁴K. S. Birdi and D. T. Vu, *J. Adhes. Sci. Technol.* **7**, 485 (1993).
- ⁵T. Ondarçuhu, T. J. Arcamone, A. Fang, H. Durou, E. Dujardin, G. Rius, and F. Perez-Murano, *Eur. Phys. J. Spec. Top.* **166**, 151 (2009).
- ⁶E. F. Hare and W. A. Zisman, *J. Phys. Chem.* **59**, 335 (1955).
- ⁷P. G. de Gennes, *Rev. Mod. Phys.* **57**, 827 (1985).
- ⁸D. Ausserré, A. M. Picard, and L. Léger, *Phys. Rev. Lett.* **57**, 2671 (1986).

- ⁹F. Heslot, N. Fraysse, and A. M. Cazabat, *Nature* **338**, 640 (1989).
- ¹⁰P. Silberzan and L. Léger, *Macromolecules* **25**, 1267 (1992).
- ¹¹A. M. Cazabat, N. Fraysse, F. Heslot, P. Levinson, J. Marsh, F. Tiberg, and M. P. Valignat, *Adv. Colloid Interface Sci.* **48**, 1 (1994).
- ¹²S. S. Sheiko, G. Eckert, G. Ignat'eva, A. M. Muzafarov, J. Spickermann, H. J. Räder, and M. Möller, *Macromol. Rapid Commun.* **17**, 283 (1996).
- ¹³M. W. J. van der Wielen, M. A. C. Stuart, and G. J. Fleer, *Langmuir* **14**, 7065 (1998).
- ¹⁴C. Bourges-Monnier and M. E. R. Shanahan, *Langmuir* **11**, 2820 (1995).
- ¹⁵T. Sekitani, Y. Noguchi, U. Zschieschang, H. Klauk, and T. Someya, *Proc. Natl. Acad. Sci. U.S.A.* **105**, 4976 (2008).
- ¹⁶C. Wingren and C. A. K. Borrebaeck, *Drug Discovery Today* **12**, 813–819 (2007).
- ¹⁷J.-U. Park, M. Hardy, S. J. Kang, K. Barton, K. Adair, D. K. Mukhopadhyay, C. Y. Lee, M. S. Strano, A. G. Alleyne, J. G. Georgiadis, and J. A. Rogers, *Nature* **6**, 782 (2007).
- ¹⁸M. Jaschke and H.-J. Butt, *Langmuir* **11**, 1061 (1995).
- ¹⁹R. D. Piner, J. Zhu, F. Xu, S. Hong, and C. A. Mirkin, *Science* **283**, 661 (1999).
- ²⁰A. Meister, S. Jeney, M. Liley, T. Akiyama, U. Staufer, N. F. de Rooij, and H. Heinzelmann, *Microelectron. Eng.* **67–68**, 644 (2003).
- ²¹A. Meister, M. Liley, J. Brugger, R. Pugin, and H. Heinzelmann, *Appl. Phys. Lett.* **85**, 6260 (2004).
- ²²J. Haaheim, R. Eby, M. Nelson, J. Fragala, B. Rosner, H. Zhang, and G. Athas, *Ultramicroscopy* **103**, 117 (2005).
- ²³Q. Tang, S.-Q. Shi, and L.-M. Zhou, *J. Nanosci. Nanotechnol.* **5**, 2167–2171 (2005).
- ²⁴A. P. Fang, E. Dujardin, and T. Ondarçuhu, *Nano Lett.* **6**, 2368–2374 (2006).
- ²⁵J. Jang, J. Sung, and G. C. Schatz, *J. Phys. Chem. C* **111**, 4648–4654 (2007).
- ²⁶O. A. Nafday, M. W. Vaughn, and B. L. Weeks, *J. Chem. Phys.* **125**, 144703 (2006).
- ²⁷J. R. Hampton, A. A. Dameron, and P. S. Weiss, *J. Am. Chem. Soc.* **128**, 1648 (2006).
- ²⁸K. Kaisei, N. Satoh, K. Kobayashi, K. Matsushige, and H. Yamada, *Nanotechnology* **22**, 17501 (2011).
- ²⁹K. Kaisei, K. Kobayashi, K. Matsushige, and H. Yamada, *Ultramicroscopy* **110**, 733 (2010).
- ³⁰K. Kaisei, K. Kobayashi, K. Matsushige, and H. Yamada, *Jpn. J. Appl. Phys.* **49**, 06GH02– (2010).
- ³¹J. P. Cleveland, S. Manne, D. Bocek, and P. K. Hansma, *Rev. Sci. Instrum.* **64**, 403 (1993).
- ³²A. Adamson and A. P. Gast, *Physical Chemistry Surfaces*, 6th ed. (Wiley-Interscience, New York, 1997).
- ³³M. Yoshimoto, T. Maeda, T. Ohnishi, H. Koinuma, O. Ishiyama, M. Shinohara, M. Kubo, R. Miura, and A. Miyamoto, *Appl. Phys. Lett.* **67**, 2615 (1995).
- ³⁴R. García, M. Calleja, and H. Rohrer, *J. Appl. Phys.* **86**, 1898 (1999).
- ³⁵R. V. Martínez, N. S. Losilla, J. Martínez, Y. Huttel, and R. García, *Nano Lett.* **7**, 1846 (2007).
- ³⁶M. G. Pollack, R. B. Fair, and A. D. Shenderov, *Appl. Phys. Lett.* **77**, 1725 (2000).
- ³⁷T. Leïchlé, D. Saya, J.-B. Pourciel, F. Mathieu, L. Nicu, and C. Bergaud, *Sens. Actuators, A* **132**, 590 (2006).
- ³⁸W. M. Wang, R. M. Stoltenberg, S. Liu, and Z. Bao, *ACS Nano* **2**, 2135 (2008).